Supporting Information

Lee et al. 10.1073/pnas.1005362107

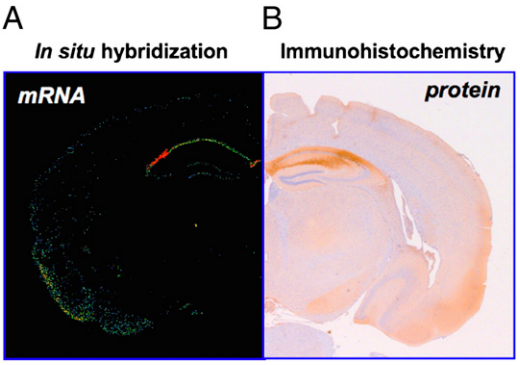

Fig. S1. RGS14 mRNA and protein expression and distribution in mouse brain. (*A*) In situ hybridization showing expression of RGS14 mRNA in mouse brain [Allen Mouse Brain Atlas (Internet). Seattle (W): Allen Institute for Brain Science, © 2009. Available from: http://mouse.brain-map.org.] (*B*) Mouse brain sections stained with anti-RGS14 monoclonal antibody (brown, DAB staining) and counterstained with hematoxylin (blue).

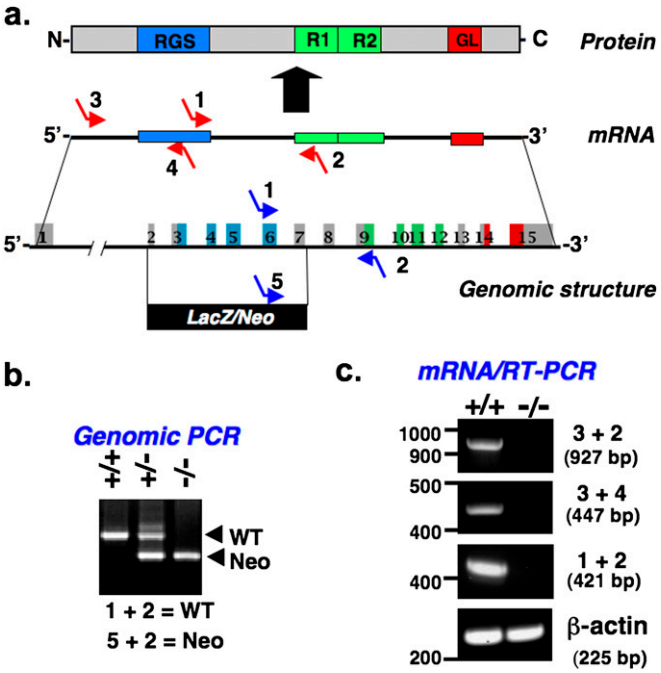

Fig. S2. Deletion of the RGS14 gene and protein in mice. (*A*) Schematic of RGS14 gene and mRNA including protein domain structures. Red arrows indicate the location of primers used in RT-PCR for mRNA. *Bottom* panel shows the structure of the genomic DNA intron and exon arrangement indicating targeting vector location and insertion site for the lacZ/neo cassette replacing exons 2 through 7. Blue arrows indicate location of primers used for PCR genotyping. (*B*) PCR genotyping. Multiplex PCR shows single larger band for wild-type genomic DNA, two bands for RGS14 (+/–) genomic DNA, and a single lower band for RGS14 (–/–) or RGS14-KO genomic DNA indicating loss of RGS14 gene and insertion of lacZ/neo cassette. Oligo pairs used for PCR are shown in *A* as blue arrows 1, 2, and 5. (*C*) RT-PCR of RGS14 mRNA from brains of WT or RGS14-KO mice. Oligo pairs used on cDNA derived from mRNA are shown in *A* as red arrows 1, 2, 3, and 4.

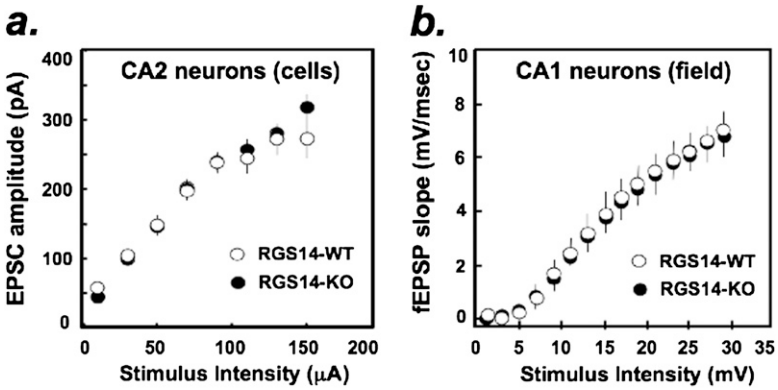

Fig. S3. Baseline synaptic transmission in wild-type and RGS14-KO mice. (*A*) Excitatory postsynaptic currents (pAs) were measured in response to varying input currents to determine baseline synaptic transmission WT (n = 3 mice, 8 neurons) RGS14-KO (n = 4 mice, 10 neurons). (*B*) For CA1 hippocampal slices, population field excitatory postsynaptic potentials (fEPSPs) output were measured in response to varying input voltages to determine baseline synaptic transmission WT (n = 10), RGS14-KO (n = 8).

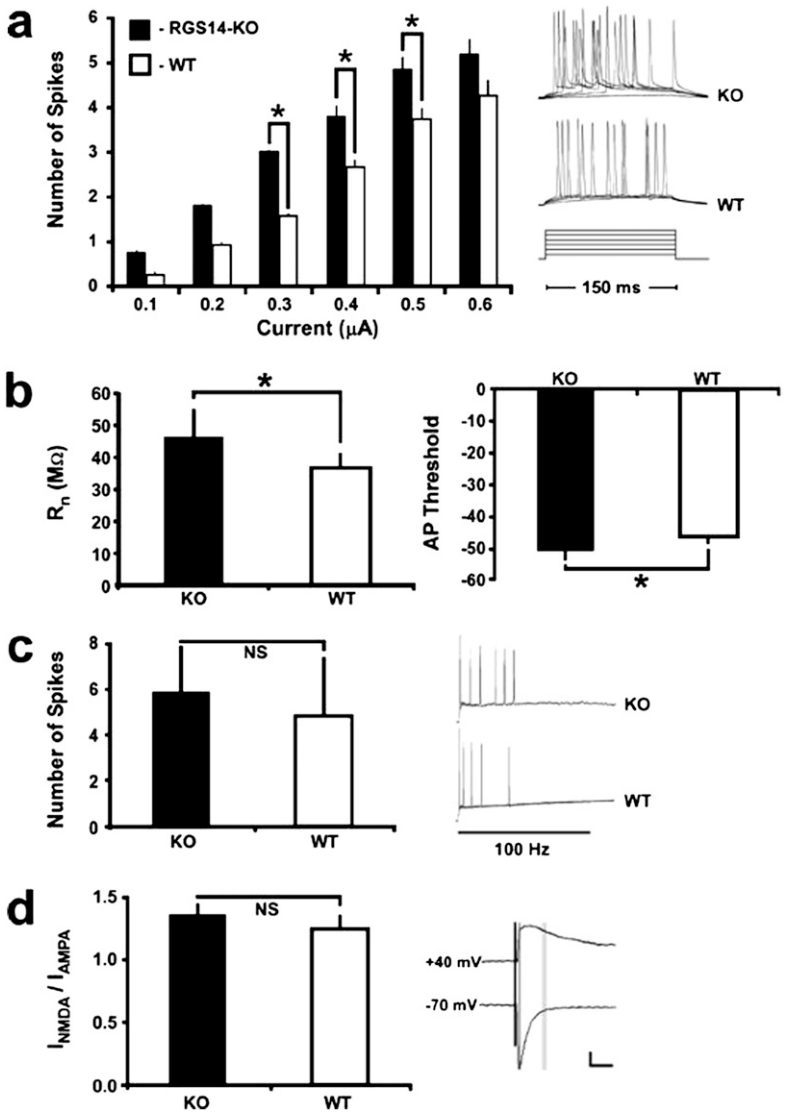

Fig. S4. CA2 neurons from RGS14-KO mice are more excitable than those from WT mice, but their synaptic properties are similar. (*A*) Average number of action potentials (spikes) evoked with 150 ms current injections in KO and WT CA2 neurons. Examples of single neuron responses and current injection waveforms are shown to the *Right*. (*B*) Average input resistances (R_n) (*Left*) and action potential thresholds (*Right*) differ between KO and WT CA2 neurons. (*C*) Average number of spikes evoked during 1 s of 100 Hz synaptic stimulation does not differ between WT and KO. Examples of representative single neuron responses are shown to the *Right*. Delivery of the 100-Hz stimulus is indicated with a bar. (*D*) Ratios of average synaptic NMDA receptor and AMPA receptor currents did not differ between neurons from WT and KO mice. Measurements of NMDA receptor and AMPA receptor-dependent components were measured at 10 and 1 ms, respectively, and are indicated by the light gray bar and dark gray bar, indicated in the examples on the *Right*, which were recorded from a single CA2 neuron from an RGS14-KO. Both measurements were acquired at +40 mV. (Scale bars, 50 pA and 50 ms.) In all panels, (*) indicates differences are statistically significant $P < 0.05$. NS, differences not significant. $N = 12$ neurons from five RGS14-KO mice and 11 neurons from four WT mice.

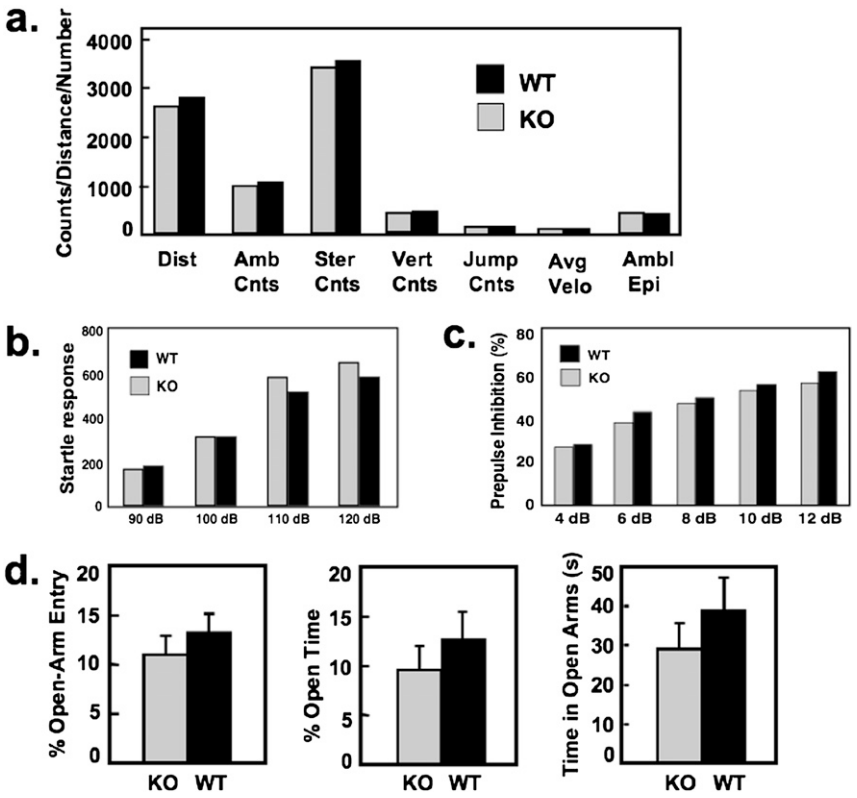

Fig. S5. (*A*) Open-field locomotor activity. Baseline motor activities were measured by examining the total ambulatory distance (in cm) during the 20-min open field test session equipped with four 24-beam infrared arrays across the base of each chamber wall. Activity data were collected via computer and analyzed with the MED Associates' Activity Monitor Data Analysis software. Motor activities measured include distance traveled (Dist), ambulatory counts (Amb cnts), stereotypy counts (Ser cnts), vertical counts (Vert. Cnts), jumping activity (Jump cnts), average velocity of movement (avg velo), and ambulatory episodes (Amb epi). Wild type (n = 34) and RGS14-KO (n = 20). (*B*) Startle response. Ten startle stimuli at each of four different startle stimulus intensities (90, 100, 110, and 120 dB) with an interstimulus interval (ISI) of 30 s. All startle stimuli were presented in a pseudorandom sequence with the constraint that each stimulus intensity occur only once in each consecutive four-trial block. Mean startle amplitudes were calculated for each mouse by computing the average startle response at each of four different startle stimulus intensities. Wild type (n = 34) and RGS14-KO (n = 20). (*C*) Prepulse inhibition of startle. Startle stimuli (115 dB, 50 ms) were presented alone or were preceded by noise prepulses (20 ms) of 2, 4, 8, 10, or 12 dB above a 63 dB white noise background (i.e., 65, 67, 71, 73, or 75 dB) with a fixed interval (100 ms) between onsets of the prepulse and startle stimuli. Five different trial types were presented in random order nine times for a total of 45 trials. Intertrial intervals ranged from 20 to 40 s. Mean startle amplitudes for the startle-alone trials and each of the five prepulse + startle trials were calculated for each mouse by averaging the startle amplitude of each trial type. Each mean prepulse + startle amplitude score was converted to a percent PPI obtained as follows: Percent PPI = 100 × (mean startle-alone amplitude − mean prepulse + startle amplitude)/(mean startle-alone amplitude). Wild type (n = 34) RGS14-KO (n = 20). (*D*) Elevated plus maze for anxiety-related behavior. Mice were placed in an elevated plus maze and closed arm entries, open arm entries, total arm entries, and time in open arms were recorded. The total number of entries (open + closed); the percent of open arm entries (open/total), and percent time in open arms (open arms time in seconds/total time 300 s). Wild type (n = 34); RGS14-KO (n = 20).